AMERICAN JOURNAL OF PHARMTECH RESEARCH

Journal home page: http://www.ajptr.com/

Anomalous dissolution behaviour of a novel amorphous form of Efavirenz

Zak Perold[1], Erna Swanepoel[1], Marius Brits[2*]

1. Research Institute for Industrial Pharmacy, North-West University, South Africa

2. WHO Collaborating Centre for the Quality Assurance of Medicines, North-West University, South Africa

ABSTRACT

This study evaluated the dissolution behaviour of a novel amorphous form (Form A) and the commercially preferred crystalline form (Form I) of efavirenz. Generally, amorphous forms tend to achieve a greater extent and rate of dissolution compared to their crystalline counterparts. The results showed that the dissolution of Form A to be significantly lower than that of Form I due to agglomeration. Factors which contributed to the agglomeration behaviour of Form A include: high surface free energy, a lower degree of wetting, and the low glass transition temperature of Form A which caused the sample to convert to the rubber phase which is stickier. The agglomeration increased the relative particle size thereby reducing the exposed surface area of Form A; ultimately reducing the rate and extent of dissolution. The dissolution behaviour of Form A was found to be dependent on sample size and surfactant (SLS) concentration. Scanning Electron Microscopy (SEM) was employed to investigate surface area properties which provided information supporting the powder dissolution results. The solubility and intrinsic behaviour of the two forms were found to be comparable. Upon further investigation it was found that Form A undergoes phase mediated transformation into Form I during the solubility and dissolution experiments and that this too contributed to the apparent dissolution and solubility behaviour of Form A. It was found the nucleation rate of Form A was potentiated by higher SLS content in the dissolution medium.

Keywords: polymorph, amorph, dissolution, solubility, efavirenz.

*Corresponding Author Email: Marius.Brits@nwu.ac.za

Received 24 January 2012, Accepted 8 February 2012

Please cite this article in press as: Perold Z *et al.*, Anomalous Dissolution Behaviour of A Novel Amorphous Form of Efavirenz. American Journal of PharmTech Research 2012.

INTRODUCTION:

Efavirenz is a non-nucleoside reverse transcriptase inhibitor (NNRTI) which acts as an inhibitor of HIV-1 reverse transcriptase[1]. It is commonly administered in combination with nucleoside reverse transcriptase inhibitors (NRTI) due to the fact that resistance towards NNRTIs has been reported[1].The use of substandard medicines result in treatment failure and increases the risk of resistantance[2,3]. Substandard medicines are products whose composition and ingredients do not meet the final product specifications[3].

A total of 19 different solid forms of efavirenz are currently described in the literature: Forms I-V, H1, α, β, y, y1, y2, ω, δ, N, O and P as well as three amorphous forms[4-8]. The literature suggests Form I to be the most desired crystal form of efavirenz for pharmaceutical manufacturing[4,5]. Different solid forms of a compound may vary in solubility and rate of dissolution due to differences in thermodynamic properties of the crystal conformations[9,10]. The more stable the crystal form, the stronger the bonding forces between the molecules will be and vice versa[10]. For dissolution to take place, the intermolecular forces of a compound must be overcome[10], and therefore rate of dissolution is indirectly proportional to crystal stability. Efavirenz is a poorly water soluble compound[11] rendering its polymorphs susceptible to significant differences in bioavailability. Theoretically meta-stable forms will exhibit higher solubility compared to their crystalline counterparts[9,10]. Amorphous forms being the least stable form of a compound are therefore anticipated to exhibit the greatest dissolution rate and extent of dissolution compared to its crystalline forms[10].

Many other aspects (besides polymorphism) contribute to product quality, including the analytical methods and specifications which are used to assess performance indicators (like dissolution). A recent study proposed how changes to the current USP dissolution medium (0.1 N HCL with 1% (w/v) Sodium Laurel Sulfate-SLS) can aid with identification of the mebendazole polymorphic forms[12]. At the time of this study, we noticed that numerous manufacturer methods, guidelines and in-process monographs state the use of either 1% or 2% SLS as dissolution medium for Efavirenz final products[13-15].

In the light of the aforementioned, we set the following objectives for this study:

i) to prepare and characterize an amorphous form of efavirenz (Form A) prepared by a quench cooling technique;

ii) to evaluate the dissolution and solubility properties of efavirenz Form A and Form I, and

iii) evaluate the difference between the use of 1% w/v or 2% w/v SLS as dissolution medium on the dissolution behaviour of both forms

MATERIALS AND METHODS

Particle size analysis

Prior to any experimental procedure, both forms (Form A and Form I) were lightly ground with the use of a mortar and pestle. The resultant powder was sieved and subjected to particle size analysis to ensure a uniform particle size distribution. Particle size distribution measurements were done with a Malvern Mastersizer 2000 (Malvern Instruments Ltd., Malvern, UK) fitted with a Hydro 2000SM dispersion unit. Samples were dispersed in the sample suspension unit containing a dispersant (water). The average d(0.5) and d(0.9) values obtained for Form I were 44 µm and 122 µm respectively. The average d(0.5) and d(0.9) values obtained for Form A were 57 µm and 123 µm. The results obtained from particle size analysis rendered the particle size of the powder used for experimental procedures to be comparable.

Diffuse Reflectance Infra-red Fourier Transform (DRIFT) spectroscopy

The IR spectra were recorded on a Nicolet Nexus 470 spectrophotometer with the Avatar diffuse reflectance smart accessory (Nicolet Instrument Corp., Madison, WI) over a range of 4000 cm^{-1}-400 cm^{-1}. IR samples were prepared and analyzed in a potassium bromide (Merck®, Johannesburg, South Africa) matrix.

X-Ray Diffractometry (XRD)

A Bruker D8-Advanced diffractometer (Bruker, Frankfurt, Germany) was used to obtain X-Ray Powder Diffraction (XRPD) patterns. The following conditions were applicable: target, Cu; voltage, 40 kV; current, 30 mA; divergence slit, 2 mm; anti-scatter slit, 0.6 mm, detector slit, 0.2 mm; monochromator; scanning speed, 2/min with a step size of 0.025 and a step time of 1.0 sec.

Differential Scanning Calorimetry (DSC)

Approximately 2-5 mg of sample was weighed into a 40 µl aluminium sample pan, fitted with a pierced lid (Mettler Toledo, Greifensee, Switzerland) and crimped. Samples were analyzed using a Mettler Toledo DSC823^e (Mettler Toledo, Greifensee, Switzerland) at a heating rate of 10°C/minute with the nitrogen flow rate set to 80 ml/min. The thermal events were evaluated by means of the STAR^e software (version 9.0x) (Mettler Toledo, Greifensee, Switzerland).

Dissolution

Two different dissolution techniques were employed to study the dissolution properties of Form A and Form I, namely: powder dissolution and intrinsic dissolution. For both techniques an

Erweka D700 dissolution system (Erweka, Heustenstamm, Germany) fitted with paddles (50 rpm) was used. 1% and 2% (w/v) SLS solutions were used as dissolution media. The dissolution experiments were performed at 37.0±0.5°C.

The samples and standards were suitably diluted and filtered before analysis. Samples were analyzed by means of (High Pressure Liquid Chromatography) HPLC as described under the High Pressure Liquid Chromatography analysis section.

Powder dissolution

The technique described by Lötter and co-workers[16] was used for the powder dissolution testing. This technique has successfully been used to distinguish between different crystal forms of different active pharmaceutical ingredients[12,17]. Samples weighing approximately 50 mg, 200 mg and 600 mg were accurately transferred into test tubes containing glass beads with a diameter of 0.1 mm (Sigma Aldrich, Johannesburg, South Africa) corresponding to approximately 50% of the sample weight. 10 ml of dissolution medium was transferred into each test tube. The suspended samples were agitated using a Vortex Genie shaker (Scientific Industries Inc., Bohemia, New York) for 30 seconds, before being rinsed into the respective vessels. Samples were withdrawn after 7.5, 15, 30 and 45 minutes. The samples were filtered using Millipore 0.45 µm filters (supplied by Microsep, Sandton, South Africa) prior to HPLC analysis.

The dissolution profiles of Form A and Form I were compared using the similarity factor[18]. The equation for the similarity factor (f_2) is depicted by equation 1. Form I was used as the reference sample.

$$f_2 = 50 \cdot \log\left\{\left[1+\frac{1}{n}\sum_{t=1}^{n}(R_t - T_t)^2\right]^{-0.5} \times 100\right\} \quad (1)$$

Where: n is the number of withdrawals; R_t is the % reference sample dissolved at time t and T_t is the % sample dissolved at time t.

Intrinsic dissolution

The intrinsic dissolution behaviour of Form A and Form I in 1% (w/v) SLS was evaluated using the guidelines described in the current United States Pharmacopeia[19] and British Pharmacopeia[20]. 300 mg samples were compressed (3 ton for 1 minute) using a Beckman 00-25 hydrolic press (Beckman, Glenrothes, Scotland) in tempered aluminum dies (diameter: 13 mm). Samples were withdrawn after 7.5, 15, 30, 60, 90, 120, 180 and 240 minutes. The samples were filtered using Millipore 0.45 µm filters (supplied by Microsep, Sandton, South Africa) and suitably diluted prior to HPLC analysis.

Solubility studies

The solubility of the two forms were determined in 0.1N HCl (pH 1.2), acetate buffer (pH 4.5), phosphate buffer (pH 6.8), 1% (w/v) SLS and 2% (w/v) SLS. Sieved fractions (approximately 200 mg) of the two forms were weighed and transferred into test tubes together with 5 ml of each medium respectively. The test tubes were sealed and affixed to sample holders in a temperature controlled water bath which was maintained at 37.0±0.2˚C. The samples were rotated at 50 rpm for 24 hours. The samples were filtered using Millipore 0.45 µm filters (supplied by Microsep, Sandton, South Africa) and suitably diluted prior to HPLC analysis.

Contact angle measurement (CAM)

Powder samples were transferred into suitable CAM sample holders. The surface of the powder bed was smoothened to ensure an even powder surface. A Krüss DSA 100S (Krüss, Hamburg, Germany) drop shape analyzer with Drop Shape Analysis for Windows, version 1.90.0.14 (Krüss, Hamburg, Germany) was used for contact angle measurements. The water drop size ranged from 7-13 µl. The sessile drop method was employed and the results were calculated using the tangent technique.

Hot stage microscopy (HSM)

A Nikon DS-Fi1 (Nikon, Tokyo, Japan) digital camera affixed to a Nikon ECLIPSE E400 light microscope (Nikon, Tokyo, Japan) was used for HSM. Samples were heated with the use of a Leitz hot stage (Leica Microsystems Inc., Bannockburn, IL). The captured images were analyzed using NIS-Elements F2.30 software (Nikon, Tokyo, Japan).

Scanning Electron Microscopy (SEM)

A small amount of sample was used to cover the carbon tape that was affixed to the pin. The sample was then covered with a gold-palladium film using an IB-2 Eiko engineering ion coater inside a vacuum (Eiko Engineering, Ibaraki, Japan). The coated sample was then affixed to the microscope sample holder and analyzed using a FEI Quanta 200 ESEM & Oxford INCA 400 EDS system (FEI, Hillsboro, OR).

High Pressure Liquid Chromatography (HPLC) analysis

The concentration of efavirenz from the dissolution and solubility samples was measured employing an isocratic HPLC method[21] on an Agilent 1200 HPLC system with Rev. B. 02.01-SR2 [260] ChemStation for LC 3D systems software (Agilent Technologies, Santa Clara, CA). A C18 (5 µm, 4.6 mm x 25 cm) column (Phenomenex, Torrance, CA) was used.

RESULT AND DISCUSSION

Preparation of the amorphous form of efavirenz

Efavirenz raw material (Matrix Laboratories Limited, Secunderabad, India), was obtained from a local pharmaceutical manufacturer. This raw material (Form I) was used as starting material for the preparation of the amorphous form by quench cooling the melt. A calibrated laboratory hot plate was covered with aluminum foil and set to 140°C. A desired amount of Form I raw material was placed onto the aluminum foil and allowed to melt. The aluminum foil was thereafter quickly removed from the hot plate and subjected to ambient conditions. The melt instantly solidified into a glassy solid. The obtained glass was dubbed efavirenz Form A. Form A was subjected to assay analysis using the method as described in the HPLC section to ensure that the employed preparation method did not result in any significant breakdown of the active. The recovery of efavirenz was found to be 99.6%.

Being an amorphous solid form, the stability of Form A was expected to be at risk. For this reason Form A was freshly prepared for each experimental procedure. The desired amount which was required for a given experimental procedure was prepared directly prior to use.

Characterization of the efavirenz crystal forms

Physico-chemical characterization by means of XRPD, DRIFT-IR and DSC was performed on the samples.

The x-ray powder diffractogram of the efavirenz raw material produced clearly defined diffraction peaks characteristic of a crystalline form (Figure 1). The presence of diffraction peaks at the following 2θ- angles: 6.0±0.2, 6.3±0.2, 10.3±0.2, 10.8±0.2, 14.1±0.2, 16.8±0.2, 20.0±0.2, 20.5±0.2, 21.10±0.2 and 24.8±0.2, confirmed the raw material to be Form I[4,5]. Form A revealed no distinct XRPD peaks (Figure 1), confirming absence of a definite crystal packing. The IR spectra of Form I and Form A differed significantly in the 2750-3500 cm^{-1} and 1600-1800 cm^{-1} regions (Figure 2). The IR spectrum of Form A did not reveal the secondary amine stretch at 3312 cm^{-1} which is prominent in the IR spectrum of Form I. Furthermore, the carbonyl stretch was observed at 1739 cm^{-1} and at 1750 cm^{-1} for Form A and Form I respectively.

The DSC thermogram of Form I revealed a melting endotherm (T_m) at 138.40˚C whilst that of Form A revealed a glass transition at 33.4˚C (T_g), a crystallization exotherm (T_c) at 83.26˚C and a melting endotherm (T_m) at 138.00˚C, when heated at a rate of 10˚C/min (Figure 3). The low T_g suggest that Form A will present in the rubber phase above this temperature and as a glass below this temperature[10].

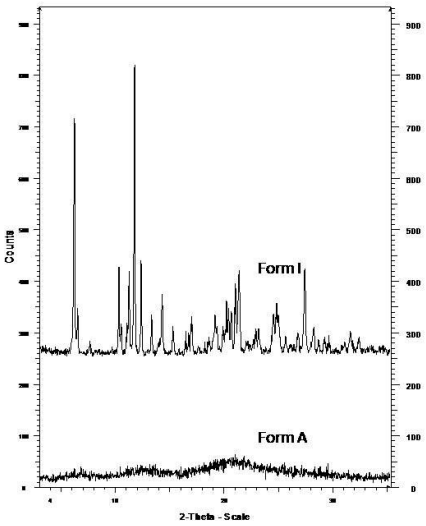

Figure 1: XRP diffractograms of efavirenz Form I and Form A.

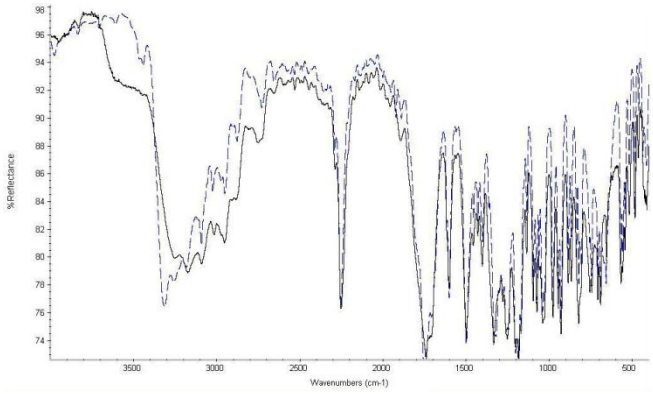

Figure 2: Overlay of the DRIFT-IR spectra of Form I (dotted) and Form A (solid).

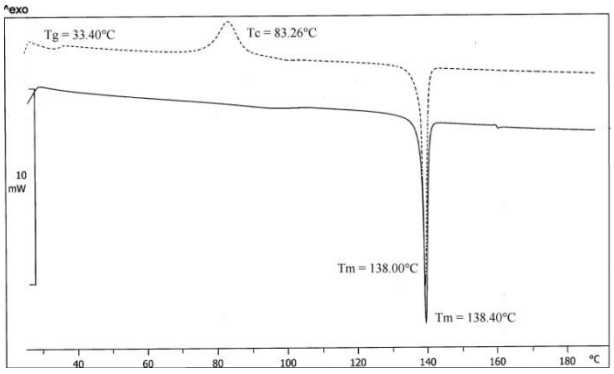

Figure 3: DSC thermograms of efavirenz Form I (solid line) and Form A (dotted line) when heated at a rate of 10˚C/min.

Hot stage microscopy (HSM) was used to elucidate and confirm the thermal events observed in the DSC thermograms of Form A and Form I. Form A revealed fine, superficial channels which formed during the preparation of the glass (Figure 4 - 1). No birefringence was detected when the sample was exposed to polarized light confirming the absence of crystalline phases in the

sample. Between 28-63°C the superficial channels disappeared and the sample displayed a smooth viscous-like surface, which could be attributed to the transition of the glass to the rubber phase. Small nuclei were detected at 76°C (Figure 4 - 3) which revealed a two dimensional growth when exposed to increased temperatures (Figure 4 - 4). Investigation of the sample at 84°C under polarized light confirmed the growth of the crystalline phase due to the presence of birefringence (Figure 4 - 6). The crystalline phase darkened at 132°C (Figure 4 - 7) and underwent complete melting at approximately 138°C (Figure 4 - 8). No remarkable HSM events were observed for Form I when exposed to increased temperatures. The melting of Form I initiated at 128°C and concluded at 135°C, confirming the single thermal event observed in the DSC thermogram thereof.

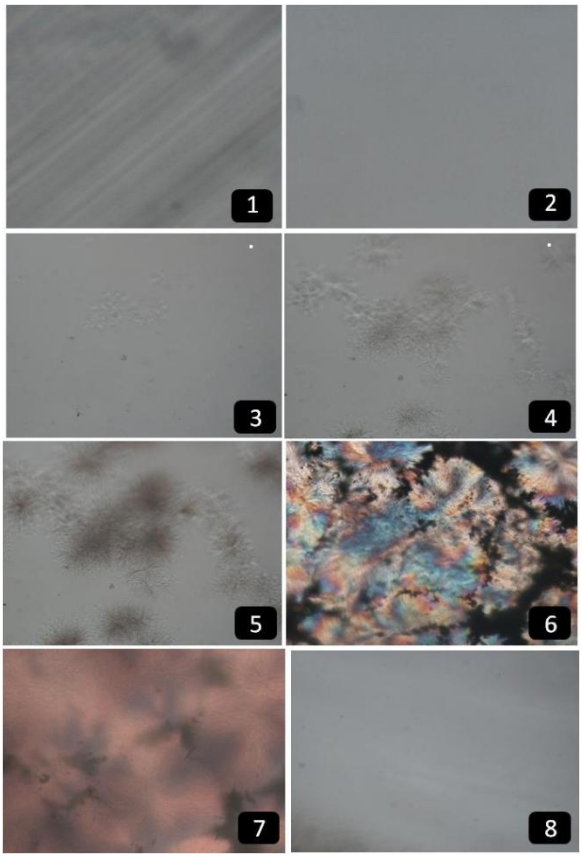

Figure 4: Hot stage photomicrographs of Form A at: (1) 15°C, (2) 55°C, (3) 76°C, (4) 79°C, (5) 80°C, (6) 84°C, (7) 132°C & (8) 138°C.

Based on the characterization techniques employed, it was clear that Form A and Form I were different solid forms of efavirenz. The study was furthered by examining the potential differences in dissolution behaviour of the two solid forms using powder and intrinsic dissolution techniques.

Powder dissolution

The objective of the powder dissolution studies was to determine potential differences in the dissolution behaviour of Form A and Form I. A two dimensional matrix approach was used for this study, evaluating the influence of variations in sample size and dissolution medium composition, on the discriminatory ability of the powder dissolution technique. The dissolution of Form A and Form I in sample sizes of 50 mg, 200 mg, and 600 mg were evaluated in 1% and 2% (w/v) SLS. The specific sample sizes were selected, as they represent the most common dosage strengths in the commercial pharmaceutical products[7]. The powder dissolution profiles are illustrated in Figure 5. The error bars included in the figures are based on ± 2 standard deviations.

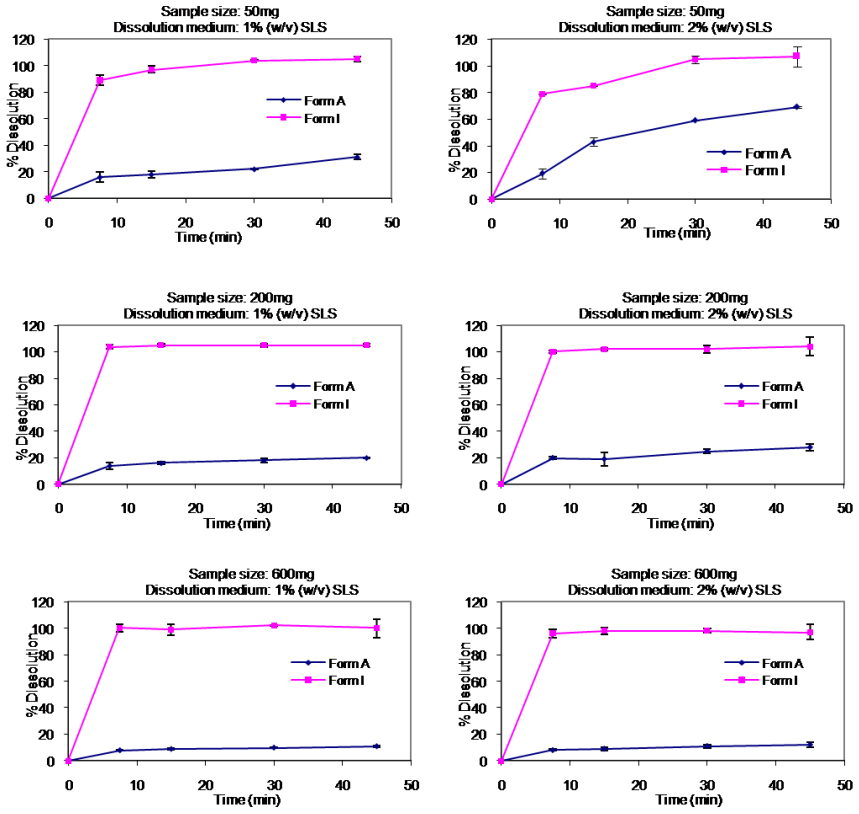

Figure 5: Dissolution profiles of Form I and Form A (sample sizes: 50 mg, 200 mg and 600 mg) in 1% and 2% (w/v) SLS respectively.

Differences in the rate and extent of dissolution of Form A and Form I were observed. Form I revealed 100% dissolution after 30 minutes regardless of the % SLS in the dissolution medium or the sample size used for the dissolution. The 50 mg dissolution profiles of Form A revealed that the extent of dissolution was approximately 2 times greater in 2% (w/v) SLS than in 1% (w/v) SLS at Q_{45min}. The difference between the Q_{45min} of Form A in 2% (w/v) and 1% (w/v)

SLS, was found to be 8% and ~0% for the 200 mg and 600 mg sample sizes respectively. The f_2-similarity factors calculated for all the profiles (Figure 6) revealed that the dissolution profiles of Form A and Form I in the various media and various sample sizes differed significantly (all $f_2 < 50$).

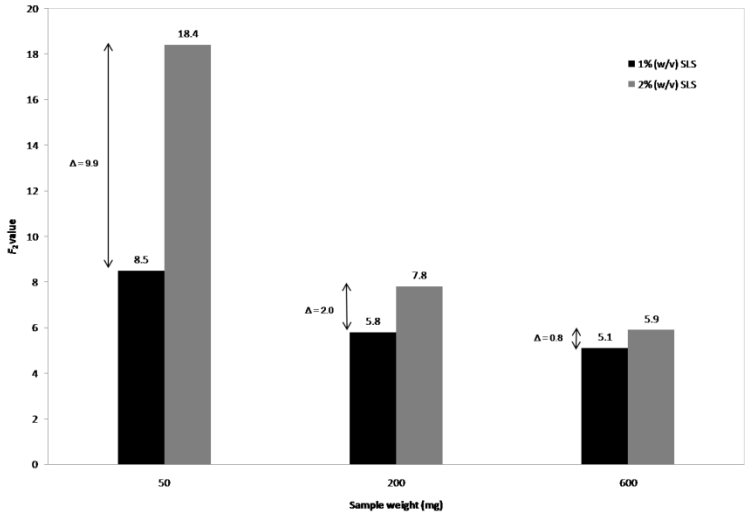

Figure 6: f_2-similarity factors calculated for the dissolution profiles of Form A and Form I using different sample sizes in 1% and 2% (w/v) SLS.

The discriminatory ability of the dissolution method was influenced by the variations in the sample size and the SLS concentration of the dissolution media (Figure 6). The effect of higher SLS concentration can predominantly be observed when comparing the 50 mg profiles in the different dissolution media. When using a sample size of 50 mg, the higher SLS content (2% SLS) resulted in a difference of 9.9 in the f_2 value when compared to the profiles in 1% SLS, however when using larger sample sizes, the higher SLS content did not significantly improve the dissolution of Form A in comparison with the dissolution behaviour thereof in 1% SLS.

Both Form A and Form I underwent agglomeration once introduced to the dissolution medium (in 1% and 2% SLS). The size of the Form A agglomerates increased with an increase in sample size, whereas the size of the Form I agglomerates remained fairly constant (Figure 7). The increased tendency towards agglomeration of Form A, increased the relative particle size of Form A, thereby reducing the exposed surface area of Form A; ultimately reducing the rate and extent of dissolution. The fact that Form I did not show an increased tendency towards agglomeration with an increase in sample size explains why much better dissolution of this form was possible. The increased tendency of Form A to form agglomerates once introduced into the medium may also be attributed to the temperature of the dissolution medium. The temperature at

which the dissolution experiments were performed (37.0±0.5°C), suggest Form A to present in the rubber phase at this temperature. The rubbery state is known to exhibit stickiness[10], which increased the tendency towards agglomeration.

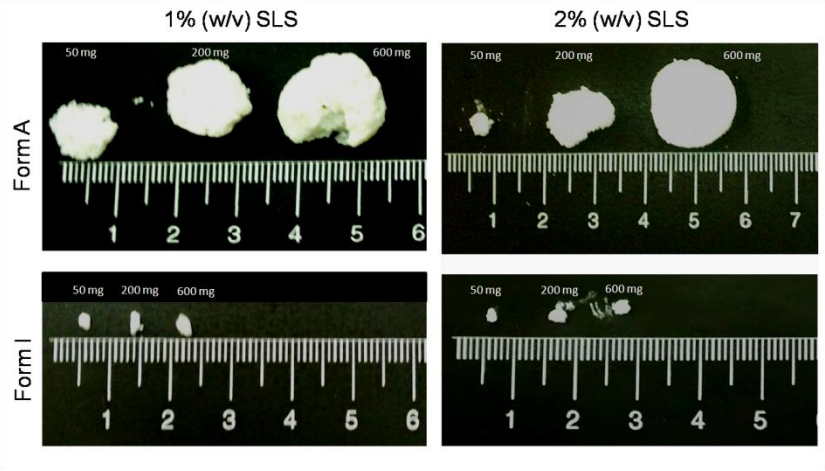

Figure 7: Typical agglomerates of Form A and Form I which formed once introduced into the dissolution media.

Although an increase in SLS content did not favour the dissolution of Form A in sample sizes of 200 mg and 600 mg in such a way as with the 50 mg sample size, the increase of SLS content did manage to potentiate the disintegration of Form A agglomerates. This observation was prominent in sample sizes of 50 and 200 mg, but less noticeable in the 600 mg sample size. Figure 8 (a) and (b) revealed that the amount of Form I dissolved after 45 minutes in both media ($C_{1\%}$ and $C_{2\%}$) was directly proportional to the sample size ($R^2 = 0.999$). The correlation between the sample size and $C_{1\%}$ or $C_{2\%}$ of Form A was diminished ($R^2 \leq 0.943$) due to the inconsistent formation and disintegration of agglomerates. The ratio of $C_{2\%}$:$C_{1\%}$ of Form A versus the sample size revealed that an increase in the SLS concentration of the medium potentiated the disintegration and dissolution of Form A. During the dissolution study it was observed that smaller agglomerates disintegrated faster compared to larger agglomerates (50 mg > 200 mg > 600 mg), elucidating the higher $C_{2\%}$ values at smaller sample sizes.

The results obtained in this study are inconsistent with anticipated behaviour of amorphous forms (i.e. improved dissolution)[10]. The dissolution behaviour of Form A can be elucidated utilizing the Noyes Whitney equation – equation 2[20].

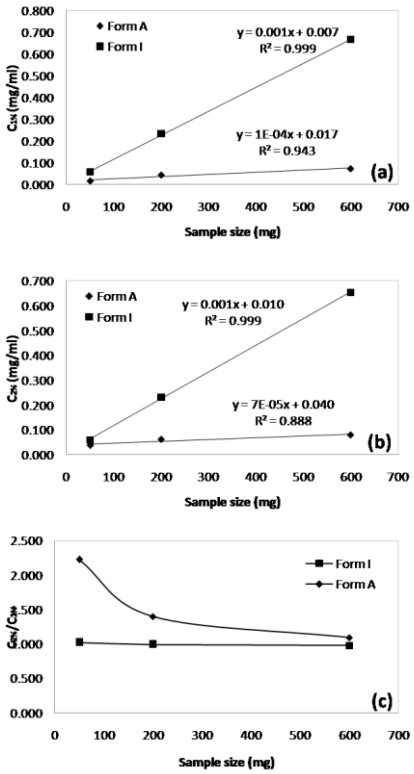

Figure 8: The amount of Form A and Form I dissolved in (a) 1% (w/v) SLS and (b) 2% (w/v) SLS after 45 minutes and (c) the ratio of the results obtained in 2% (w/v) SLS and 1% (w/v) SLS.

$$\frac{dm}{dt} = kA(C_s - C) \qquad (2)$$

Where $\frac{dm}{dt}$ is the dissolution rate, k the dissolution rate constant, A the surface area of the dissolving solid, C_s the concentration of the solid in the dissolution medium and C the concentration of the solid in the diffusion layer surrounding the solid.

The Noyes Whitney equation reveals that the dissolution rate is dependant on surface area (A) and solubility ($C_s - C$) of the solid. We investigated the solubility and surface area properties (by CAM and SEM) of the two forms in order to evaluate the potential influences these properties may have on the dissolution behaviour.

Solubility

Forms A and I were subjected to 24 hour solubility experiments in aqueous physiological- (0.1 N HCl pH 1.2, acetate buffer pH 4.5 and phosphate buffer pH 6.8) and non-physiological (1% (w/v) and 2% (w/v) SLS) media. The solubility results in the physiological media were extremely low, which corresponded well with the findings of Rowe *et al.*[23]. The solubility of efavirenz Form A and Form I in 1% and 2% (w/v) SLS are reported in Table 1. The increase in

the SLS concentration of the medium caused a two fold increase in the solubility of the two forms. The solubility ratios for Forms A and I in 1% and 2% (w/v) SLS ranged between 1.0 and 1.2, indicating that the solubility of Form A and Form I in the mentioned media did not differ significantly. Anomalous behaviour of amorphous forms has been reported in the literature where the amorphous forms revealed a lower/same solubility compared to their crystalline counterparts[17,24,25].

Table 1. The solubility (δ) of efavirenz Form I (I) and Form A (A) in 1% and 2% (w/v) SLS respectively at 37.0±0.2°C after 24 hours

	1 % (w/v) SLS	2% (w/v) SLS	$\delta^{2\%}/\delta^{1\%}$
Form A	$\delta_A^{1\%}$=11.02 ± 0.16 mg/ml	$\delta_A^{2\%}$=21.1 ± 0.27 mg/ml	$\delta_A^{2\%}/\delta_A^{1\%}$=2.1
Form I	$\delta_I^{1\%}$= 9.11 ± 0.83 mg/ml	$\delta_I^{2\%}$= 22.3 ± 1.29 mg/ml	$\delta_I^{2\%}/\delta_I^{1\%}$= 2.5
δ_A/δ_I	$\delta_A^{1\%}/\delta_I^{1\%}$=1.2	$\delta_A^{2\%}/\delta_I^{2\%}$=1.0	

Due to the fact that the equilibrium solubility was determined after 24 hours, the similarity in the solubilities of the two forms could have been attributed to the conversion of Form A to Form I in the aqueous media. The powder residue from the solubility experiments were subjected to further analysis (see phase mediated transformation section).

Wettability

Since wetting of a solid is the precursor to the dissolution process, it is understandable that differences in wettability will result in differences in dissolution rate. Contact angle measurements are commonly used to evaluate the extent of wettability and are often capable of elucidating differences in the crystal surface properties of polymorphic forms, making it possible to explain differences in dissolution behaviour[26,27].

The contact angles of Form A (θ=135.1±0.5°) and Form I (θ=113.2±0.2°) were calculated using the tangent method and the circle fill method – Figure 9. The results obtained from both methods were in agreement. The higher contact angle of Form A signifies a higher surface free energy of the solid and a lower degree of wetting compared to that of Form I. It has been reported that cohesive energy of a substance is directly proportional to the surface free energy of the solid[28]. CAM findings thus supports why the tendency of agglomeration was more prominent with Form A in comparison with Form I. Common techniques (such as interactive mixing, sonication and

vortexing with glass beads) that are employed to decrease the effect of agglomeration during powder dissolution are not always successful[28], as was the case with this study. The lower extent of wettability and high extent of agglomeration contributed to the lower dissolution of Form A when compared to Form I.

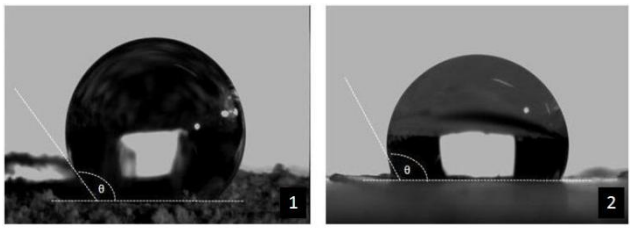

Figure 9: The contact angles of: 1) Form A (θ=135.1±0.5°) and 2) Form I (θ=113.2±0.2°).

Scanning electron microscopy (SEM)

SEM was used to compare the surface area properties of Form A and Form I. The SEM photomicrographs are depicted in Figure 10. The SEM photomicrograph of Form A revealed shapeless, plate-like particles with dense, smooth surfaces whereas Form I presented particles with varying morphology and prominent layering characteristics. The layered structure of Form I allowed for a greater surface area exposed to the dissolution medium, which benefitted its dissolution more than the morphology of Form A.

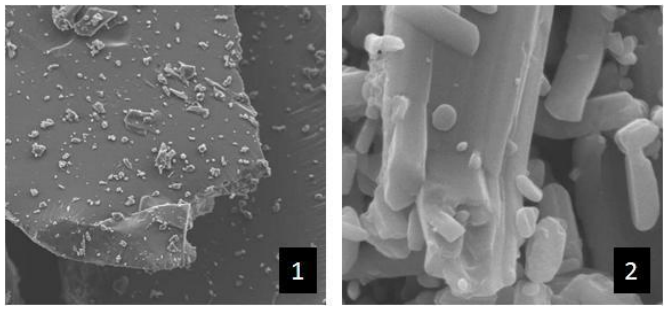

Figure 10: SEM photomicrographs of Form A (1) and Form I (2).

It can thus be concluded that the significant differences in the powder dissolution of Form A and Form I, could be attributed to the differences in the surface area properties of the two forms.

Intrinsic Dissolution

Intrinsic dissolution studies were performed on Form A and Form I in order to evaluate the dissolution behaviour with a constant surface area, thus minimizing the effect of surface properties and agglomeration. The intrinsic dissolution results of Form A and Form I are depicted in Figure 11.

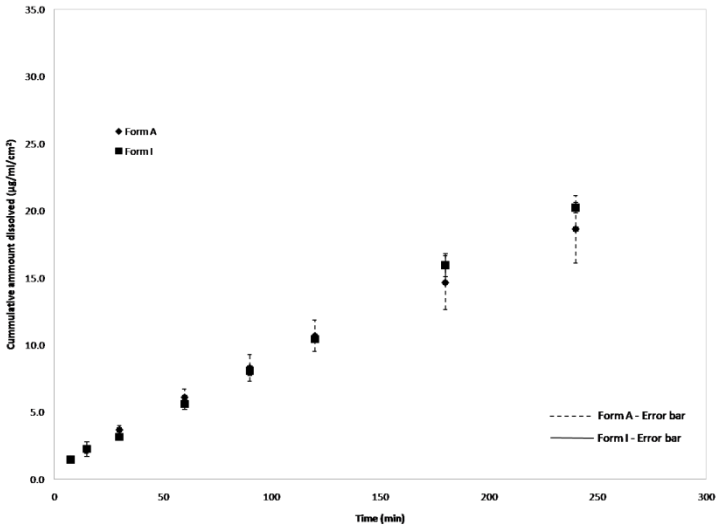

Figure 11. The intrinsic dissolution of Form A and Form I dissolved versus time in 1% (w/v) SLS at 37.0±0.5°C.

To ensure sink conditions during the intrinsic dissolution studies, the minimum dissolution medium volumes (V_{min}) were calculated for Form A and Form I using equation 3[29].

$V_{min} = (W \times 10)/ \delta$ (3)

Where V_{min} is the minimum dissolution medium volume required, W is the weight of the sample and δ the solubility of the form in the specific dissolution[29].

V_{min} was calculated for Form A and Form I, and found to be 272 ml and 329 ml respectively. Thus, the 900 ml dissolution medium volume that was used during this study was adequate to ensure sink conditions. The absence of a plato (Figure 11) confirmed the sink conditions.

Upon completion of the study it was observed that the surfaces of the Form A compacts revealed prominent, white encrustments (Figure 12). It has been reported that dissolution may induce a solvent mediated phase transformation of meta-stable crystal phases[30]. We investigated this possibility by performing DSC and XRPD analysis on these encrustments (refer to phase mediated transformation section).

Phase mediated transformation

Analysis of the powder remnants from the solubility and dissolution experiments by XRPD revealed that Form A had converted into Form I during these experiments. The XRPD no longer depicted a halo shape, but instead revealed the presence of the most prominent peaks characteristic of Form I (see section characterisation).

DSC is commonly employed to quantify amorphous content[31,32], and for this reason such a method was similarly developed to quantify Form A. Binary mixtures of Form A and I were

prepared and analysed by DSC. The difference in recrystallisation energy allowed for the linear calibration curve (Figure 13), which made it possible to calculate unknown concentrations of Form A from the dissolution and solubility samples.

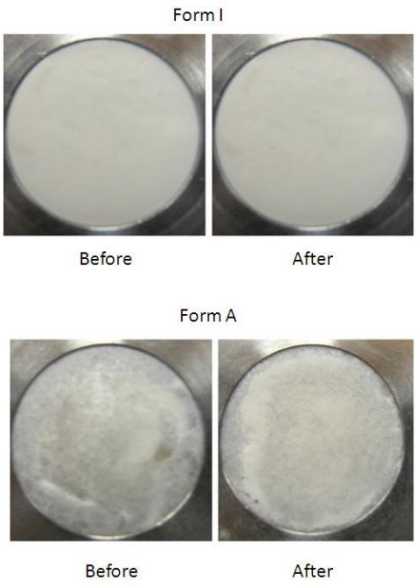

Figure 12: Appearance of the Form A & Form I compacts prior- and after the intrinsic dissolution studies revealed the prominent, white encrustments formed on the surface of the Form A compacts.

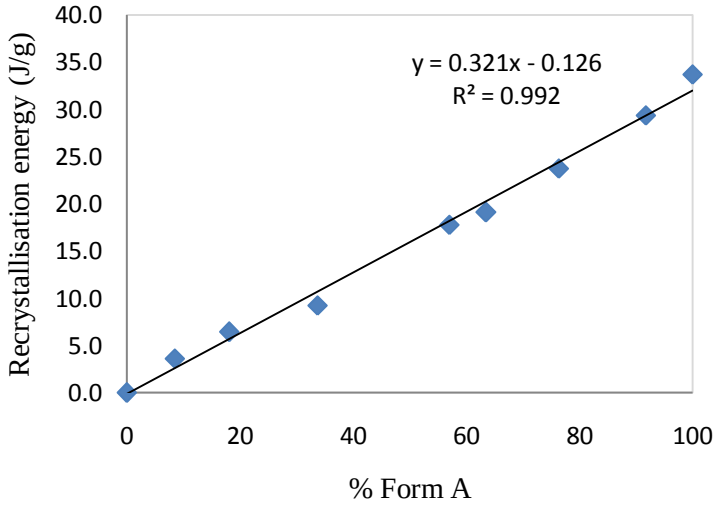

Figure 13: The relationship between recrystallization energy and theoretical % Form A.

The powder remnants from the solubility experiments after 24 hours revealed that Form A had completely transformed in Form I (% Form I ~ 100%) as the DSC thermogram did not present with a recrystallisation peak (recrystallisation energy = 0 J/g). The solubility of Form A, and its influence on the powder dissolution thereof, is therefore dependent on the rate and extent of the

conversion into Form I. The mediated phase transition of Form A during the solubility experiment elucidates the similarities in the solubility behaviour of Form A and Form I. The analysis of the white encrustments from the intrinsic dissolution experiments revealed that the exposed surface (encrustments) isolated from the compacts had completely transformed into Form I (% Form I ~ 100%) as the DSC thermogram did not present with a recrystallisation peak (recrystallisation energy = 0 J/g). The mediated phase transition of Form A elucidates the similarities in the intrinsic dissolution profiles of Form A and Form I. From Figure 11 and Table 2, it was clearly observed that the margin of error for the intrinsic dissolution of Form A increased over time. At the start of the dissolution, the margin of error is minuscule; however it intensified and reached a maximum of 2.5 µg/ml.cm^2 at the final withdrawal time. This error margin (error range) indicated that the phase transition of Form A was inconsistent amongst all the samples (vessels) and that the accuracy of the results was influenced by the varying rate and extent of phase transition.

Table 2.Intrinsic dissolution rates of Form A and Form I in 1% (w/v) SLS at 37.0±0.5°C

Form	Equation	r^2	Intrinsic dissolution rate (µg.min^{-1}.cm^{-2})	Error range (µg.ml^{-1}.cm^{-2})
A	y = 0.0735x + 1.393	0.997	0.074	0.1 – 2.5
I	y = 0.0817x + 0.815	0.999	0.082	0.1 – 0.9

The powder dissolution conditions were simulated in the same fashion as previously described, but instead of evaluating the % dissolved, we analysed the remaining powder from the vessels at the original withdrawal times, by DSC. These results (Figure 14) show that a linear relationship (R^2 > 0.990) was obtained for the phase transformation of Form A into Form I over time for the different sample sizes. These results not only made it possible to predict the extent of transformation at any given time, but also showed that the phase transformation was influenced by the agglomeration/sample size, as the phase transformation rate was found to be indirectly proportional to sample size (Figure 15). The DSC analyses of the powder samples of Form A from the powder dissolutions in 2% w/v SLS revealed that it had completely converted to Form I from 7.5 minutes regardless of the sample size.

The solubility and dissolution results obtained for Form A is not a true reflection of the behaviour of Form A, seeing that this form underwent a phase mediated transformation. It is known that surfactants (like SLS) may promote the nucleation process during the phase mediated transformation[33]. This study supports this hypothesis, seeing that the powder dissolution of Form A in 2% SLS revealed a faster transition (and dissolution) compared to that in 1% SLS.

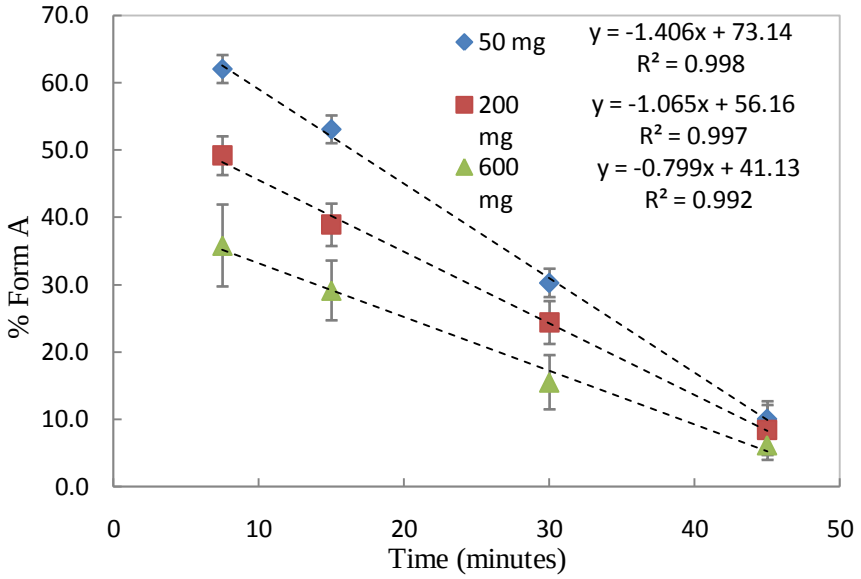

Figure 14: The % Form A at specific time intervals during powder dissolution experiments in 1% SLS for different sample sizes.

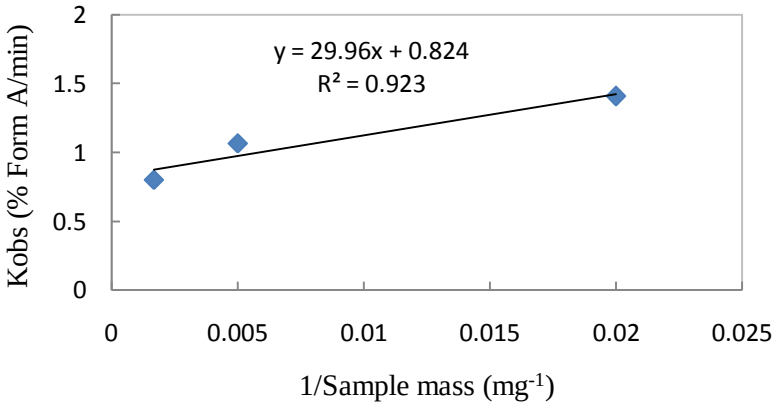

Figure 15. The relationship between the rate of phase transformation (K_{obs}) and sample size (mg^{-1}).

CONCLUSION:

An amorphous form of efavirenz (Form A) was successfully prepared by means of a quench cooling technique. Form A and the preferred polymorphic form of efavirenz (Form I), were characterized and thereafter subjected to powder dissolution, intrinsic dissolution, solubility testing, CAM and SEM analyses to evaluate the possible differences between these two forms.

Form A underwent agglomeration once introduced into the dissolution media, which limited the dissolution thereof, causing significant differences between the dissolution profiles of Form A and Form I (f_2 value < 50). The degree of the agglomeration was found to be proportional to an increase in sample size. Using higher levels of SLS potentiated the dissolution performance of

Form A in smaller sample sizes, as increased SLS content in the dissolution medium promoted the disintegration of the agglomerates at the smaller sample size. CAM and SEM supplemented the findings of the powder dissolution results.

Intrinsic dissolution and solubility studies were performed in an attempt to elucidate the findings of the powder dissolution studies. The results from the intrinsic dissolution and solubility studies showed no significant differences between Form A and Form I. Further study into the behaviour of Form A revealed it to be susceptible to phase mediated transformation in the dissolution media. It was found the transformation of Form A to be potentiated when using smaller sample sizes and higher SLS content.

Agglomeration and thermodynamic instability are unwanted characteristics during and after product manufacture which may influence the quality of a final product and ultimately the effectiveness of treatment. The use of Form A during manufacturing is discouraged.

REFERENCES:

1. Safrin S. Antiviral Agents. In, Katzung BG(ed). Basic & Clinical Pharmacology. 8th ed., New York, NY: McGraw-Hill Companies Inc; 2001; 823-44.
2. Werthemeier AI, Norris J. Safeguarding against substandard/counterfeit drugs: Mitigating a macroeconomic pandemic. Res Soc Adm Pharm 2009; 5:4-16.
3. Newton PN, Green MD, Fernandez M. Impact of poor-quality medicines in the 'developing' world. Trends Pharmacol Sci 2009; 31:99-101.
4. Clarke W, Crocker LS, Kukura JL. Process for the crystallization of reverse transcriptase inhibitor using an anti-solvent. Patent WO 98/33782 1998;29p.
5. Radesca LA, Maurin MB, Rabel SR, Moore, JR. Crystalline efavirenz. Patent WO 99/64405 1999;72p.
6. Reddy BP, Rathnakar K, Reddy RR, Reddy MD & Reddy, KS. Novel polymorphs of Efavirenz. Patent US 2006/0235008A1 2006;6p.
7. Doney JA. Amorphous efavirenz and the production thereof. Patent US 2007/0026073A1 2007;16p.
8. Sharma R, Bhusan KH, Aryan RC, Singh N, Pandya B, Kumar Y. Polymorphic forms of Efavirenz and processes for their preparation. Patent WO 2006/040643A2 2006;49p.
9. Bauer J, Spanton S, Henry R, Quick J, Dziki W, Porter W, Morris J. Ritonavir: An extraordinary example of conformational polymorphism. Pharm Res 2001; 18(6):859-66.

10. Buckton G. Solid-state properties. In Aulton ME(ed.) Pharmaceutics: The science of dosage form design. New York, NY: Churchill Livingstone; 2001; 141-52.
11. Gao JZH, Hussain MA, Motheram R, Gray, DAB, Benedek IH, Fiske WD, Doll WJ, Sandefer E, Page RC & Digenis GA. Investigation of human pharmaco scintigraphic behaviour of two tablets and a capsule formulation of a high dose poorly water soluble/highly permeable drug (Efavirenz). J Pharm Sci 2007; 96: 2970-77.
12. Swanepoel E, Liebenberg W, de Villiers MM. Quality evaluation of generic drugs by dissolution test: changing the USP dissolution medium to distinguish between active and non-active Mebendazole polymorphs. Eur J Pharm Biopharm 2003; 55: 345-49.
13. WHO.int [Internet]. World Health Organization online resources [updated 2010 Sep; cited 2012 Jan 12]. Available online at http://www.who.int/medicines/services/expertcommittees/pharmprep/EfavirenzTabs_QAS10-355Rev1_01102010.pdf
14. FDA.gov [Internet]. US Food and Drug Administration – Dissolution methods [cited 2012 Jan 12]. Available online at http://www.accessdata.fda.gov/scripts/cder/dissolution/dsp_SearchResults_Dissolutions.cfm?PrintAll=1
15. USP.org [Internet]. United States Pharmacopeial convention. Efavirenz capsules pending monograph version 1 [updated 2009; cited 2012 Jan 12]. Available online at http://www.usp.org/pdf/EN/pendingStandards/m4047.pdf
16. Lötter AP, Flanagan DR, Palepu NR, Guillory JK. A simple reproducible method for determining dissolution rates of hydrophobic powders. Pharm Tech 1983; April: 59-66.
17. Henwood SQ, Liebenberg W, Tiedt LR, Lötter AP, de Villiers MM. Characterization of the solubility and dissolution properties of several new rifampicin polymorphs, solvates and hydrates. Drug Dev Ind Pharm 2001; 27(10):1017-30.
18. Moore JW, Flanner HH. Mathematical comparison of dissolution profiles. Pharm Tech 1996; June: 64-68.
19. USPNF.com [Internet]. United States Pharmacopeia online. [Updated 2012; cited 2012 Jan 12]. Available online at http://www.uspnf.com
20. Pharmacopeia.co.uk [Internet]. British Pharmacopeia online [updated 2012; cited 2012 Jan 12]. Available online at http://www.pharmacopeia.co.uk

21. USP.org [Internet]. United States pharmacopeial convention. Authorize USP Salmous standards version 1. [Updated 2007; cited 2012 Jan 12]. Available online at http://www.usp.org/pdf/EN/international/efavirenz.pdf
22. Aulton ME. Dissolution and solubility. In Aulton ME (ed.) Pharmaceutics: The science of dosage form design. 2nd ed., New York, NY: Churchill Livingstone; 2002; 15-32.
23. Rowe S, Fontalbert L, Rabel S, Maurin M. Physical chemical properties of efavirenz. Aapsj.org [Internet]. American Association of Pharmaceutical Sciences Journal [updated 1999; cited 2012 Jan 12]. Available from http://www.aapsj.org/abstracts/AM_1999/1005.htm
24. Hancock BC, York P, Rowe RC. The use of solubility parameters in pharmaceutical dosage form design. Int J Pharm 1997; 148: 1-21.
25. Henwood SQ, Liebenberg W, Tiedt LR, Lötter AP & de Villiers MM. Characterization of the solubility and dissolution properties of several new rifampicin polymorphs, solvates and hydrates. Drug Dev Ind Pharm 2001; 27(10):1017-30.
26. Buckton G (1993) Assessment of the wet ability of pharmaceutical powders. J Adh Sci Technol 1993; 7(3): 205-19.
27. Kiesvaara J, Yliruusi J, Ahomäki E (1993) Contact angles and surface free energies of theophylline and salicylic acid powders determined by the Washburn method. Int J Pharm 1993; 97:101-09.
28. De Villiers MM. Influence of agglomeration of cohesive particles on the dissolution behavior of furosemide powder. Int J Pharm 1996; 136:175-79.
29. Fahmy R, Marnane B, Bensley & Hollenback RG. Dissolution test development for complex veterinary dosage forms: oral boluses. AAPS PharmSci 2001; 4:4 article 35.
30. Garcia E, Veesler S, Biostelle R. & Hoff H (1999) Crystallization and dissolution of pharmaceutical compounds: An experimental approach. J cryst growth 1999; 198/199: 1360-64.
31. Lappalainen M, Pitkänen I, Harjunen P. Quantification of low levels of amorphous content in sucrose by hyper DSC. Int J Pharm 2006; 307:150-55.
32. Lefort R, De Gusseme A, Willart JF, Danède F, Descamps M. Solid state NMR and DSC methods for quantifying the amorphous content in solid dosage forms: an application to ball-milling of trehalose. Int J Pharm 2004; 280:209-19.
33. Šehić S, Betz G, Hadžidedić S, El-Arini SK, Leuenberger H. Investigation of intrinsic dissolution behaviour of different carbamazepine samples. Int J Pharm 2010; 386: 77-90.